



New Look at $\psi(4160)$ and $\psi(4230)$

----Could they be the same state?

周智勇
东南大学

Arxiv: 2304.07052,
in collaboration with Chun-Yong Li and Zhiguang Xiao

2023年8月28日，中国科学院大学，雁栖湖



目录

outline

01 Motivation

02 Simplest Friedrichs model

03 General Friedrichs-Lee-QPC scheme

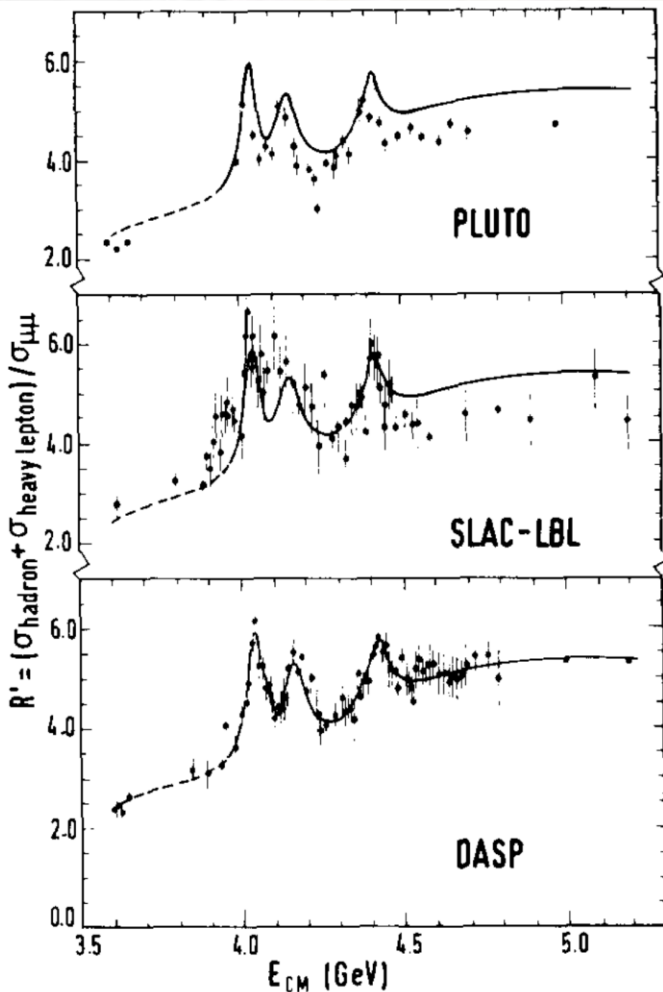
04 Numerical studies of $e^+e^- \rightarrow \bar{D}D, \bar{D}D^*, \bar{D}^*D^*, D\bar{D}\pi$ cross section data

05 Conjectures about $\psi(4160)$ and $\psi(4230)$

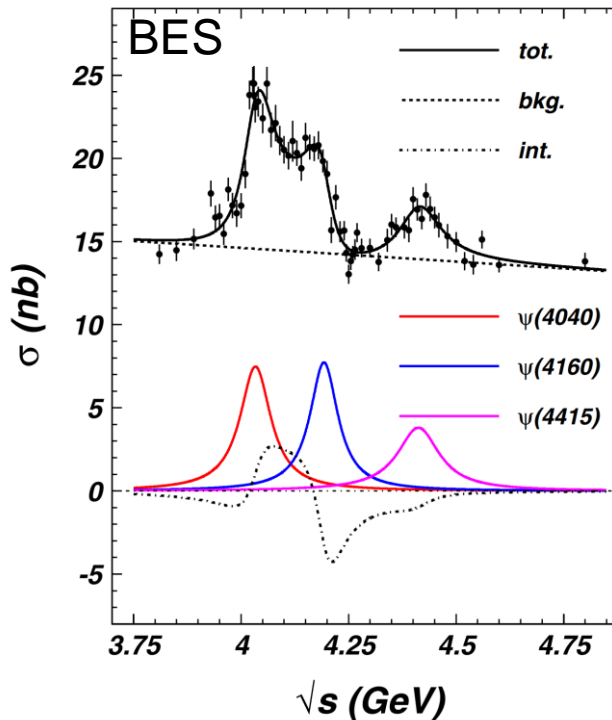


Motivation

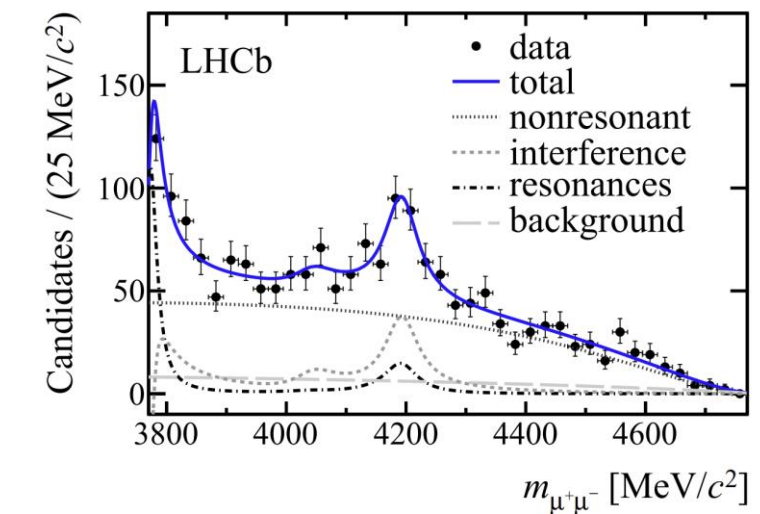
Experiment status of $\psi(4160)$



PLB. 76 (1978) 361



PRD. 82 (2010) 077501



PRL 111 (2013) 11, 112003

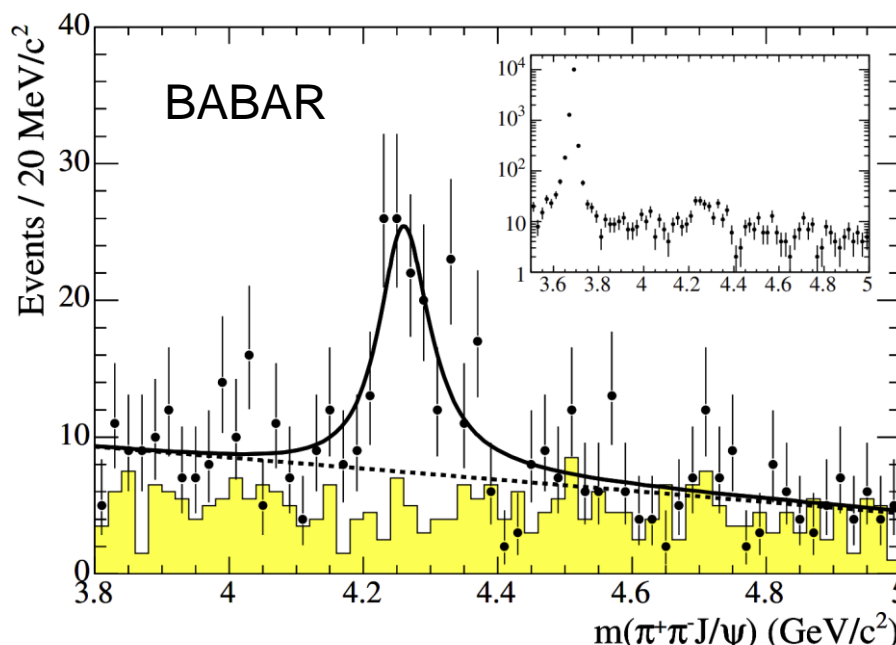


Experiment status of $\psi(4160)$

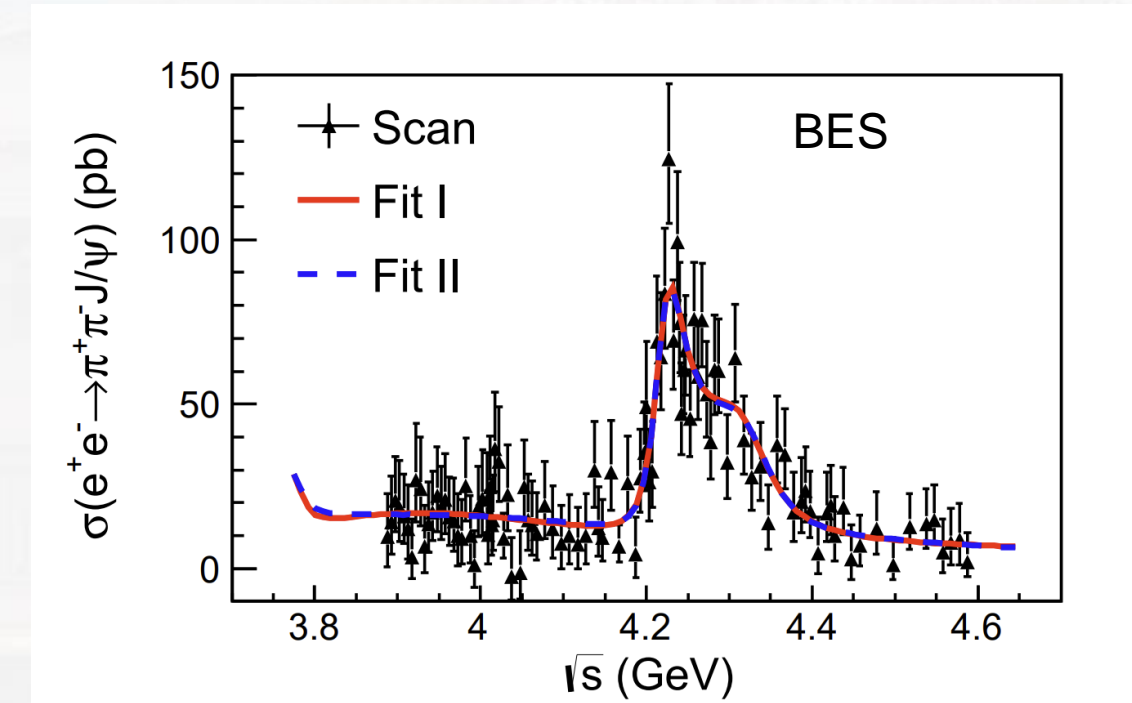
VALUE (MeV)	DOCUMENT ID	TECN	COMMENT
4191 ± 5 OUR AVERAGE			
4191 ⁺⁹ ₋₈	AAIJ	2013BC LHCb	$B^+ \rightarrow K^+ \mu^+ \mu^-$
4191.7 ± 6.5	¹ ABLIKIM	2008D BES2	$e^+ e^- \rightarrow \text{hadrons}$
	• • We do not use the following data for averages, fits, limits, etc. • •		
4193 ± 7	² MO	2010 RVUE	$e^+ e^- \rightarrow \text{hadrons}$
4151 ± 4	³ SETH	2005A RVUE	$e^+ e^- \rightarrow \text{hadrons}$
4155 ± 5	⁴ SETH	2005A RVUE	$e^+ e^- \rightarrow \text{hadrons}$
4159 ± 20	BRANDELIK	1978C DASP	$e^+ e^-$



Experiment status of $\psi(4230)$



PRL. 95 (2005) 142001



PRL. 118 (2017) 9, 092001



Experiment status of $\psi(4230)$

VALUE (MeV)	EVTS	DOCUMENT ID	TECN	COMMENT
4222.5 ± 2.4	OUR AVERAGE Error includes scale factor of 1.7. See the ideogram below.			
$4221.4 \pm 1.5 \pm 2.0$		¹ ABLIKIM	2022AM BES3	$e^+ e^- \rightarrow \pi^+ \pi^- J/\psi$
$4225.3 \pm 2.3 \pm 21.5$		² ABLIKIM	2022AU BES3	$e^+ e^- \rightarrow K^+ K^- J/\psi$
$4234.4 \pm 3.2 \pm 0.2$		³ ABLIKIM	2021AJ BES3	$e^+ e^- \rightarrow \pi^+ \pi^- \psi(2S)$
$4216.7 \pm 8.9 \pm 4.1$		⁴ ABLIKIM	2020AG BES3	$e^+ e^- \rightarrow \mu^+ \mu^-$
$4220.4 \pm 2.4 \pm 2.3$		⁵ ABLIKIM	2020N BES3	$e^+ e^- \rightarrow \pi^0 \pi^0 J/\psi$
$4218.6 \pm 3.8 \pm 2.5$		⁵ ABLIKIM	2020O BES3	$e^+ e^- \rightarrow \eta J/\psi$
$4218.5 \pm 1.6 \pm 4.0$		⁶ ABLIKIM	2019AI BES3	$e^+ e^- \rightarrow \omega \chi_{c0}$
$4228.6 \pm 4.1 \pm 6.3$		ABLIKIM	2019R BES3	$e^+ e^- \rightarrow \pi^+ D^0 D^{*-} + \text{c.c.}$
$4200.6^{+7.9}_{-13.3} \pm 3.0$		⁷ ABLIKIM	2019V BES3	$e^+ e^- \rightarrow \gamma \chi_{c1}(3872)$
$4218^{+5.5}_{-4.5} \pm 0.9$		ABLIKIM	2017G BES3	$e^+ e^- \rightarrow \pi^+ \pi^- h_c$
• • We do not use the following data for averages, fits, limits, etc. • •				
$4231.9 \pm 5.3 \pm 4.9$		ABLIKIM	2020N BES3	$e^+ e^- \rightarrow \pi^0 Z_c(3900)^0, Z_c^0 \rightarrow \pi^0 J/\psi$
$4222.0 \pm 3.1 \pm 1.4$		⁸ ABLIKIM	2017B BES3	$e^+ e^- \rightarrow \pi^+ \pi^- J/\psi$
$4209.5 \pm 7.4 \pm 1.4$		⁹ ABLIKIM	2017V BES3	$e^+ e^- \rightarrow \pi^+ \pi^- \psi(2S)$
$4209.1 \pm 6.8 \pm 7.0$		¹⁰ ZHANG	2017B RVUE	$e^+ e^- \rightarrow \pi^+ \pi^- \psi(2S)$
$4223.3 \pm 1.6 \pm 2.5$		¹¹ ZHANG	2017C RVUE	$e^+ e^- \rightarrow \pi^+ \pi^- J/\psi \text{ or } \psi(2S)$
$4230 \pm 8 \pm 6$	180	¹² ABLIKIM	2015C BES3	$e^+ e^- \rightarrow \omega \chi_{c0}$
$4258.6 \pm 8.3 \pm 12.1$		¹³ LIU	2013B BELL	$e^+ e^- \rightarrow \gamma \pi^+ \pi^- J/\psi$
$4245 \pm 5 \pm 4$		¹⁴ LEES	2012AC BABR	$10.58 e^+ e^- \rightarrow \gamma \pi^+ \pi^- J/\psi$
$4247 \pm 12^{+17}_{-32}$		^{15, 13} YUAN	2007 BELL	$10.58 e^+ e^- \rightarrow \gamma \pi^+ \pi^- J/\psi$
$4284^{+17}_{-16} \pm 4$	13.6	HE	2006B CLEO	$9.4 - 10.6 e^+ e^- \rightarrow \gamma \pi^+ \pi^- J/\psi$
$4259 \pm 8^{+2}_{-6}$	125	¹⁶ AUBERT,B	2005I BABR	$10.58 e^+ e^- \rightarrow \gamma \pi^+ \pi^- J/\psi$



Experiment status of $\psi(4230)$

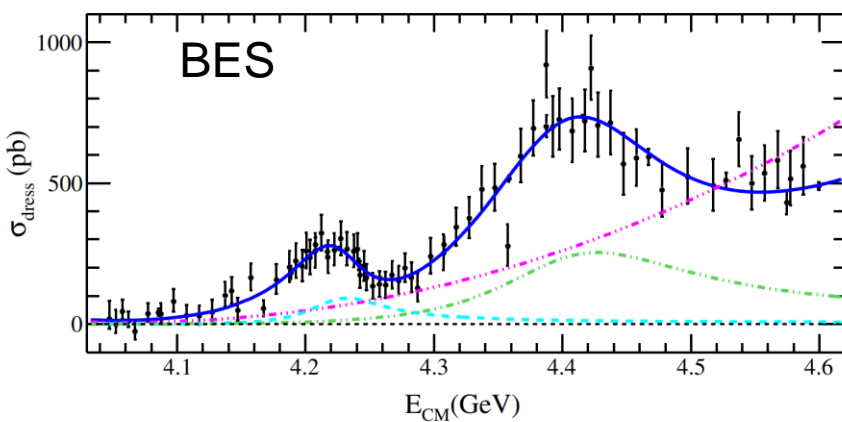


FIG. 2. Fit to the dressed cross section of $e^+e^- \rightarrow \pi^+ D^0 D^{*-}$, where the black dots with error bars are the measured cross sections and the blue line shows the fit result. The error bars are statistical only. The pink dashed triple-dot line describes the phase-space contribution, the green dashed double-dot line describes the R_2 contribution, and the light blue dashed line describes the R_1 contribution.

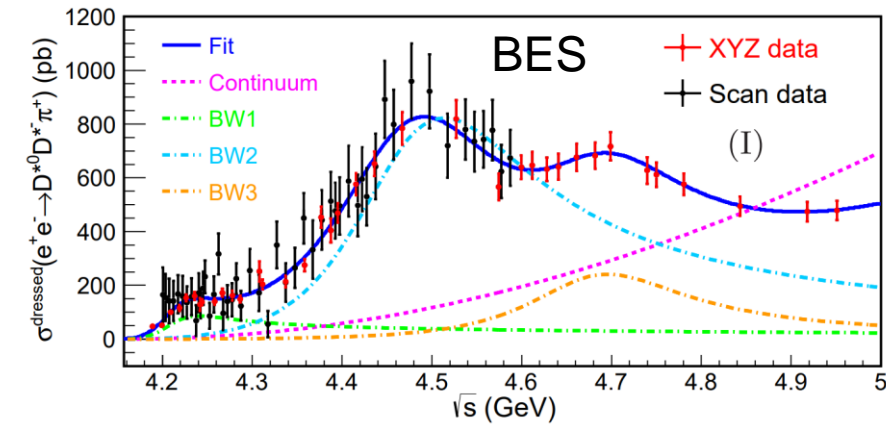


FIG. 3. The fit results (solution I) of the dressed cross section line shape of $e^+e^- \rightarrow D^{*0} D^{*-} \pi^+$. The black and red points with error bars are data, including statistical and systematic uncertainties. The blue curve is the total fit. The green, azure and orange dashed curves describe three BW functions, and the pink dashed curve is the three body phase space contribution.

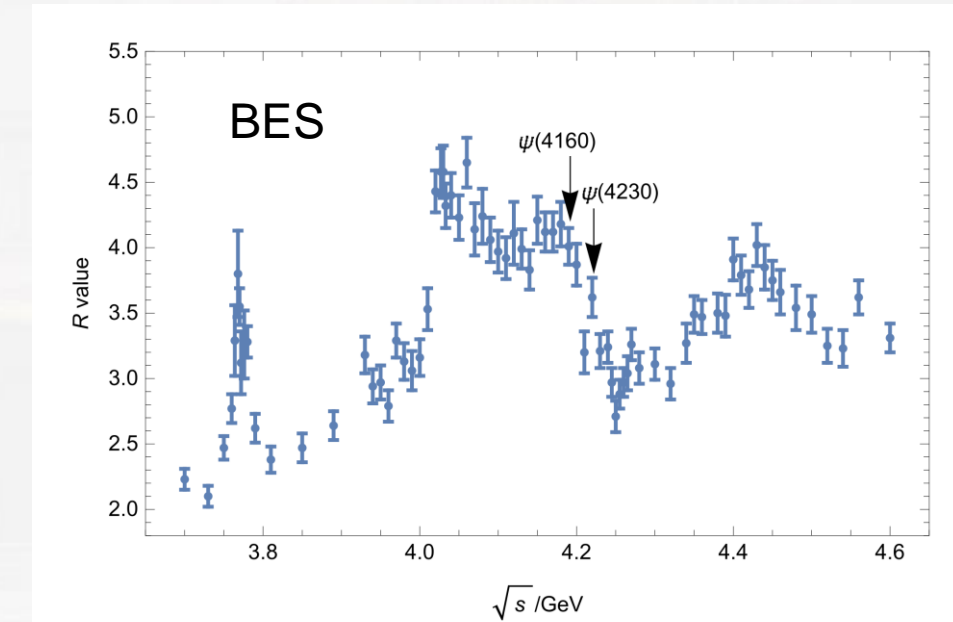


Motivation

$\psi(4160)$ and $\psi(4230)$

- Both of them are 1^{--} states, small mass splitting, similar widths
- Hardly accommodated in the quark models simultaneously
- Mutually exclusive decay modes
 - $\psi(4160)$ mainly open-charm modes
 - $\psi(4230)$ mainly hidden-charm modes, except $\pi^+ D^0 D^{*-}$ and $D^{*0} D^{*-} \pi^+$
- No same decay mode has been reported.

	$\psi(4160)$	$\psi(4230)$
Mass	4191 ± 5 MeV	4222.5 ± 2.4 MeV
Width	70 ± 10 MeV	48 ± 8 MeV





Motivation

$\psi(4160)$

VALUE(MeV)	DOCUMENT ID	TECN	COMMENT
4191 ± 5	OUR AVERAGE		
4191 ⁺⁹ ₋₈	AAIJ	2013BC LHCb	$B^+ \rightarrow K^+ \mu^+ \mu^-$
4191.7 ± 6.5	¹ ABLIKIM	2008D BES2	$e^+ e^- \rightarrow \text{hadrons}$
• • We do not use the following data for averages, fits, limits, etc. • •			
4193 ± 7	² MO	2010 RVUE	$e^+ e^- \rightarrow \text{hadrons}$
4151 ± 4	³ SETH	2005A RVUE	$e^+ e^- \rightarrow \text{hadrons}$
4155 ± 5	⁴ SETH	2005A RVUE	$e^+ e^- \rightarrow \text{hadrons}$
4159 ± 20	BRANDELIK	1978C DASP	$e^+ e^-$
<i>Mode</i>		Fraction (Γ_i / Γ)	Scale Factor/ Conf. Level
Γ_1	$e^+ e^-$	$(6.9 \pm 3.3) \times 10^{-6}$	2096
Γ_2	$\mu^+ \mu^-$	seen	2093
Γ_3	$D\bar{D}$	seen	956
Γ_4	$D^0 \bar{D}^0$	seen	956
Γ_5	$D^+ D^-$	seen	947
Γ_6	$D^* \bar{D} + \text{c.c.}$	seen	798
Γ_7	$D^*(2007)^0 \bar{D}^0 + \text{c.c.}$	seen	802
Γ_8	$D^*(2010)^+ D^- + \text{c.c.}$	seen	792
Γ_9	$D^* \bar{D}^*$	seen	592
Γ_{10}	$D^*(2007)^0 \bar{D}^*(2007)^0$	seen	604
Γ_{11}	$D^*(2010)^+ D^*(2010)^-$	seen	592
Γ_{12}	$D^0 D^- \pi^+ + \text{c.c.} \text{ [excl. } D^*(2007)^0 \bar{D}^0 + \text{c.c., } D^*(2010)^+ D^- + \text{c.c.}]$	not seen	
Γ_{13}	$D\bar{D}^* \pi + \text{c.c.} \text{ (excl. } D^* \bar{D}^* \text{)}$	seen	
Γ_{14}	$D^0 D^+ \pi^- + \text{c.c.} \text{ (excl. } D^*(2010)^+ D^*(2010)^- \text{)}$	not seen	
Γ_{15}	$D_s^+ D_s^-$	not seen	719
Γ_{16}	$D_s^{*+} D_s^{*-} + \text{c.c.}$	seen	385

$\psi(4230)$

VALUE(MeV)	EVTS	DOCUMENT ID	TECN	COMMENT
4222.5 ± 2.4	OUR AVERAGE	Error includes scale factor of 1.7. See the ideogram below.		
4221.4 ± 1.5 ± 2.0		¹ ABLIKIM	2022AM BES3	$e^+ e^- \rightarrow \pi^+ \pi^- J/\psi$
4225.3 ± 2.3 ± 21.5		² ABLIKIM	2022AU BES3	$e^+ e^- \rightarrow K^+ K^- J/\psi$
4234.4 ± 3.2 ± 0.2		³ ABLIKIM	2021AJ BES3	$e^+ e^- \rightarrow \pi^+ \pi^- \psi(2S)$
4216.7 ± 8.9 ± 4.1		⁴ ABLIKIM	2020AG BES3	$e^+ e^- \rightarrow \mu^+ \mu^-$
4220.4 ± 2.4 ± 2.3		⁵ ABLIKIM	2020N BES3	$e^+ e^- \rightarrow \pi^0 \pi^0 J/\psi$
4218.6 ± 3.8 ± 2.5		⁵ ABLIKIM	2020O BES3	$e^+ e^- \rightarrow \eta J/\psi$
4218.5 ± 1.6 ± 4.0		⁶ ABLIKIM	2019AI BES3	$e^+ e^- \rightarrow \omega \chi_{c0}$
4228.6 ± 4.1 ± 6.3		ABLIKIM	2019R BES3	$e^+ e^- \rightarrow \pi^+ D^0 D^{*-} + \text{c.c.}$
4200.6 ^{+7.9} _{-13.3} ± 3.0		⁷ ABLIKIM	2019V BES3	$e^+ e^- \rightarrow \gamma \chi_{c1}(3872)$
4218 ^{+5.5} _{-4.5} ± 0.9		ABLIKIM	2017G BES3	$e^+ e^- \rightarrow \pi^+ \pi^- h_c$
• • We do not use the following data for averages, fits, limits, etc. • •				
4231.9 ± 5.3 ± 4.9		ABLIKIM	2020N BES3	$e^+ e^- \rightarrow \pi^0 Z_c(3900)^0, Z_c^0 \rightarrow \pi^0 J/\psi$
4222.0 ± 3.1 ± 1.4		⁸ ABLIKIM	2017B BES3	$e^+ e^- \rightarrow \pi^+ \pi^- J/\psi$
4209.5 ± 7.4 ± 1.4		⁹ ABLIKIM	2017V BES3	$e^+ e^- \rightarrow \pi^+ \pi^- \psi(2S)$
4209.1 ± 6.8 ± 7.0		¹⁰ ZHANG	2017B RVUE	$e^+ e^- \rightarrow \pi^+ \pi^- \psi(2S)$
4223.3 ± 1.6 ± 2.5		¹¹ ZHANG	2017C RVUE	$e^+ e^- \rightarrow \pi^+ \pi^- J/\psi \text{ or } \psi(2S)$
4230 ± 8 ± 6	180	¹² ABLIKIM	2015C BES3	$e^+ e^- \rightarrow \omega \chi_{c0}$
4258.6 ± 8.3 ± 12.1		¹³ LIU	2013B BELL	$e^+ e^- \rightarrow \gamma \pi^+ \pi^- J/\psi$
4245 ± 5 ± 4		¹⁴ LEES	2012AC BABR	10.58 $e^+ e^- \rightarrow \gamma \pi^+ \pi^- J/\psi$
4247 ± 12 ⁺¹⁷ ₋₃₂		^{15, 13} YUAN	2007 BELL	10.58 $e^+ e^- \rightarrow \gamma \pi^+ \pi^- J/\psi$
4284 ⁺¹⁷ ₋₁₆ ± 4	13.6	HE	2006B CLEO	9.4 – 10.6 $e^+ e^- \rightarrow \gamma \pi^+ \pi^- J/\psi$
4259 ± 8 ⁺² ₋₆	125	¹⁶ AUBERT,B	2005I BABR	10.58 $e^+ e^- \rightarrow \gamma \pi^+ \pi^- J/\psi$



How to describe a resonance

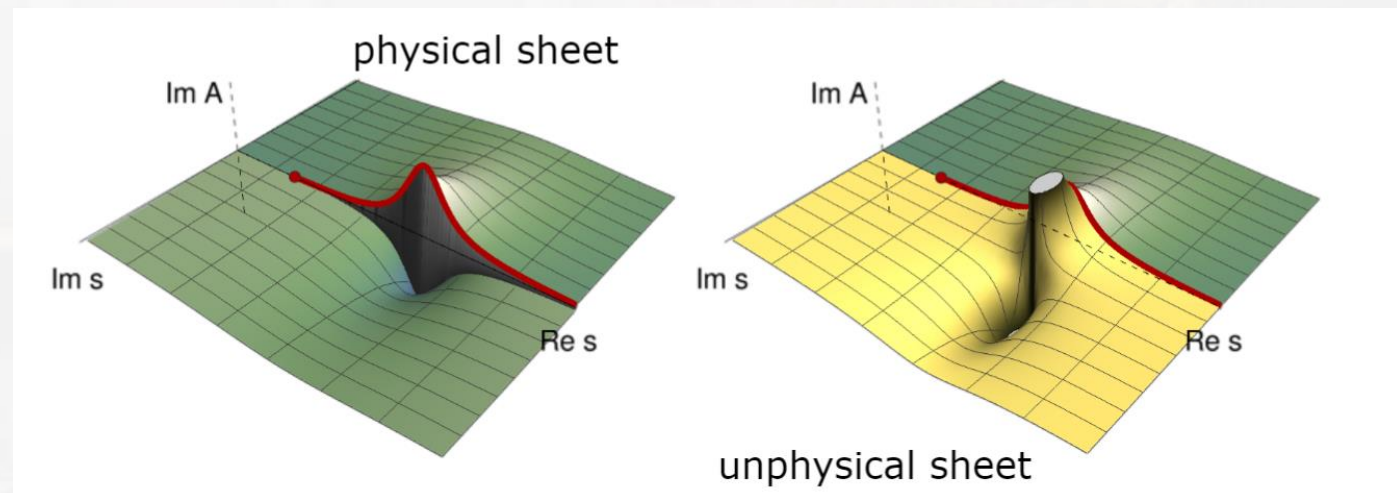
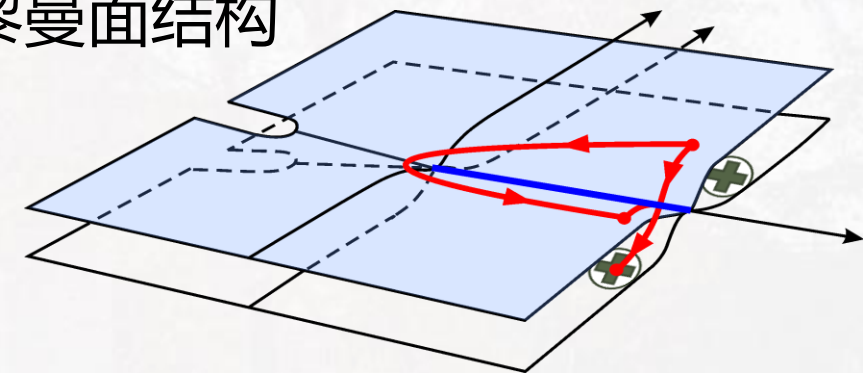
$$\begin{aligned} & \langle p'_1 p'_2, b | iT | p_1 p_2, a \rangle \\ &= i(2\pi)^4 \delta^4(p_1 + p_2 - p'_1 - p'_2) \mathcal{M}(p_1, p_2; p'_1, p'_2)_{ba} \end{aligned}$$

$$\text{Disc } \mathcal{M}_{ba} = \mathcal{M}_{ba} - \mathcal{M}_{ab}^* = i(2\pi)^4 \sum_c \int d\Phi_c \mathcal{M}_{cb}^* \mathcal{M}_{ca}$$

$$Im \mathcal{M}_{ba} = \sum_c \mathcal{M}_{cb}^* \rho_c \mathcal{M}_{ca}$$

Unitarity and analyticity

黎曼面结构

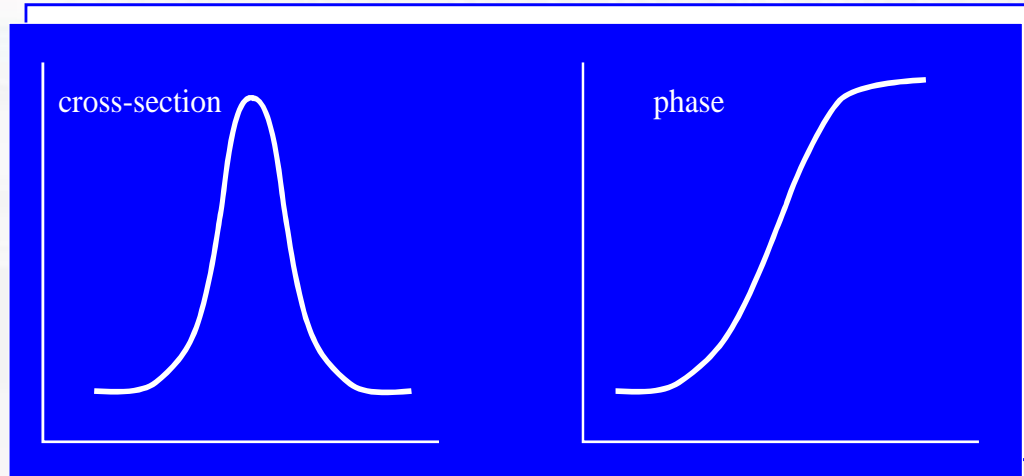




How to describe a resonance

The simplest Breit-Wigner

$$T = \frac{1}{M^2 - s - i M \Gamma}$$



Or Breit-Wigner distribution with energy-dependent width

$$T_l(s) = \frac{B_l^2(q)\Gamma}{M^2 - m^2 - i \rho B_l^2(q)m_0\Gamma}$$

$$B_l(q, q_R) = \frac{F_l(q)}{F_l(q_R)}, \rho_i = \frac{2q_i}{m}$$

Blatt-Weisskopf Barrier Factors

$$F_0(x) = 1$$

$$F_1(x) = \sqrt{\frac{x}{x+1}}$$

$$F_2(x) = \sqrt{\frac{13x^2}{(x-3)^2 + 9x}}$$

.....

by Hippel and Quigg (1972)



A lesson from Taylor' s book

The behavior of the partial cross section $\sigma_l(p)$,

$$\sigma_l(p) = \frac{4\pi(2l+1)}{p^2} \sin^2 \delta_l(p)$$

near a resonance depends on the value of the background δ_{bg} . Four different possibilities are shown in Fig. 13.3. The first and simplest, shown as the curves below (a), is when the background δ_{bg} is zero, and $\delta(p)$ therefore

242

13. Resonances

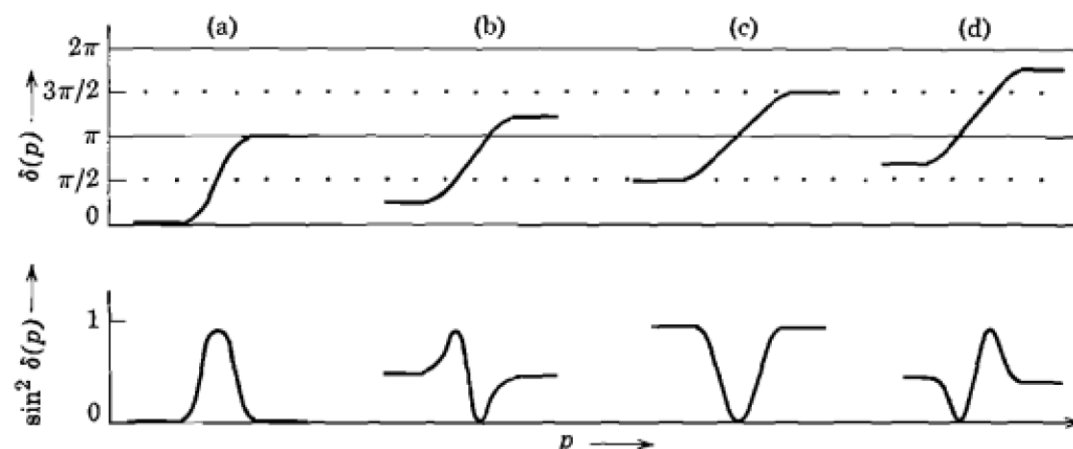


FIGURE 13.3. Four possible resonances. The $\delta(p)$ plots show the resonant phase shifts for $\delta_{bg} = 0, \pi/4, \pi/2$, and $3\pi/4$. The $\sin^2 \delta(p)$ plots show the corresponding behavior of the partial cross section [apart from a factor $4\pi(2l+1)/p^2$].

J.R.Taylor,
Scattering theory,
P241-242



What we should know about Breit-Wigner distribution in the experimental analysis

- Only distribution, no analyticity
- Multi-solution ambiguity

$n + 1$ Breit-Wigner with 2^n solutions
of similar fit quality

K. Zhu et. al., IJMPA 26, 4511 (2011)

A. D. Bokin, arXiv:0710.5627

X. Han and C. P. Shen, CPC 42, 043001 (2018)

Y. Bai and D. Chen, PRD 99, 072007

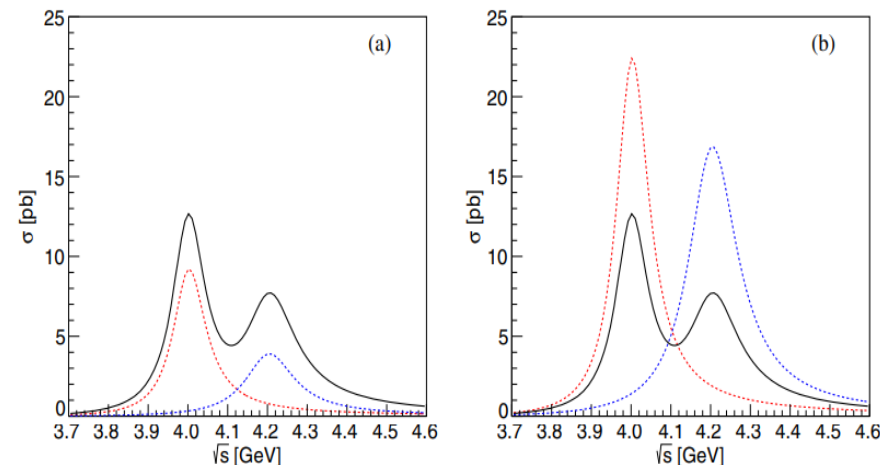


FIG. 2. An example of interference between two Breit-Wigner distributions. The solid curve is the total cross section, and the dashed curves are the individual contributions from the resonances.



What we should know about Breit-Wigner distribution in the experimental analysis

- **Only distribution, no analyticity**
- **Multi-solution ambiguity**
- **Non-unitarity**



Coupled-channel models with unitarity

- E. Eichten, K. Gottfried, T. Kinoshita, K. Lane, and T.-M. Yan, Phys.Rev. D 21, 203 (1980)
- N. A. Tornqvist, Z. Phys. C 68, 647 (1995)
- H.-B. Li, X.-S. Qin, and M.-Z. Yang, Phys. Rev. D 81, 011501 (2010)
- X. Cao and H. Lenske, Hadron 2019, pp. 433–437, arXiv:1408.5600
- A. Limphirat, W. Sreethawong, K. Khosonthongkee, and Y. Yan, Phys. Rev. D 89, 054030 (2014)
- N. N. Achasov and G. N. Shestakov, Phys. Rev. D 86, 114013 (2012)
- Y.-J. Zhang and Q. Zhao, Phys. Rev. D 81, 034011 (2010)
- J. Segovia, D. R. Entem, and F. Fernandez, Phys. Rev. D 83, 114018 (2011)
- T. V. Uglov, Y. S. Kalashnikova, A. V. Nefediev, G. V. Pakhlova, and P. N. Pakhlov, JETP Lett. 105, 1 (2017)
- T. Wolkanowski, F. Giacosa, and D. H. Rischke, Phys. Rev. D 93, 014002 (2016), arXiv:1508.00372
- Z. Yang, G.-J. Wang, J.-J. Wu, M. Oka, and S.-L. Zhu, Phys. Rev. Lett. 128, 112001 (2022)
- S. X. Nakamura, Q. Huang, J. J. Wu, H. P. Peng, Y. Zhang, and Y. C. Zhu, Phys.Rev.D 107 (2023) 9, L091505
- Z.-L. Zhang, Z.-W. Liu, S.-Q. Luo, F.-L. Wang, B. Wang, and H. Xu, Phys. Rev. D 107, 034036 (2023)
-



Motivation

A method to restore the unitarity----K matrix

$$S = 1 + 2i A$$

$$A = K(1 - iK)^{-1}$$

$$K_{ij} = \sum_{\alpha} G_{i\alpha}(s) \frac{1}{M_{\alpha}^2 - s} G_{j\alpha}(s)$$

$$G_{i\alpha}^2(s) = g_{i\alpha}^2 \frac{k_i^{2l_i+1}}{\sqrt{s}} \theta(s - s_i)$$

$$A_{ij} = \sum_{\alpha\beta} G_{i\alpha}(s) P_{\alpha\beta}(s) G_{j\beta}(s)$$

$$(P^{-1}(s))_{\alpha\beta} = (M_{\alpha}^2 - s)\delta_{\alpha\beta} - i \sum_m G_{m\alpha} G_{m\beta}$$

33 free parameters to fit well $e^+e^- \rightarrow D\bar{D}, D\bar{D}^*, D^*\bar{D}^*$, $D\bar{D}\pi$, but no poles' informations could be extracted.

Uglov et al., JETP Lett. 105, 1 (2017), arXiv:1611.07582

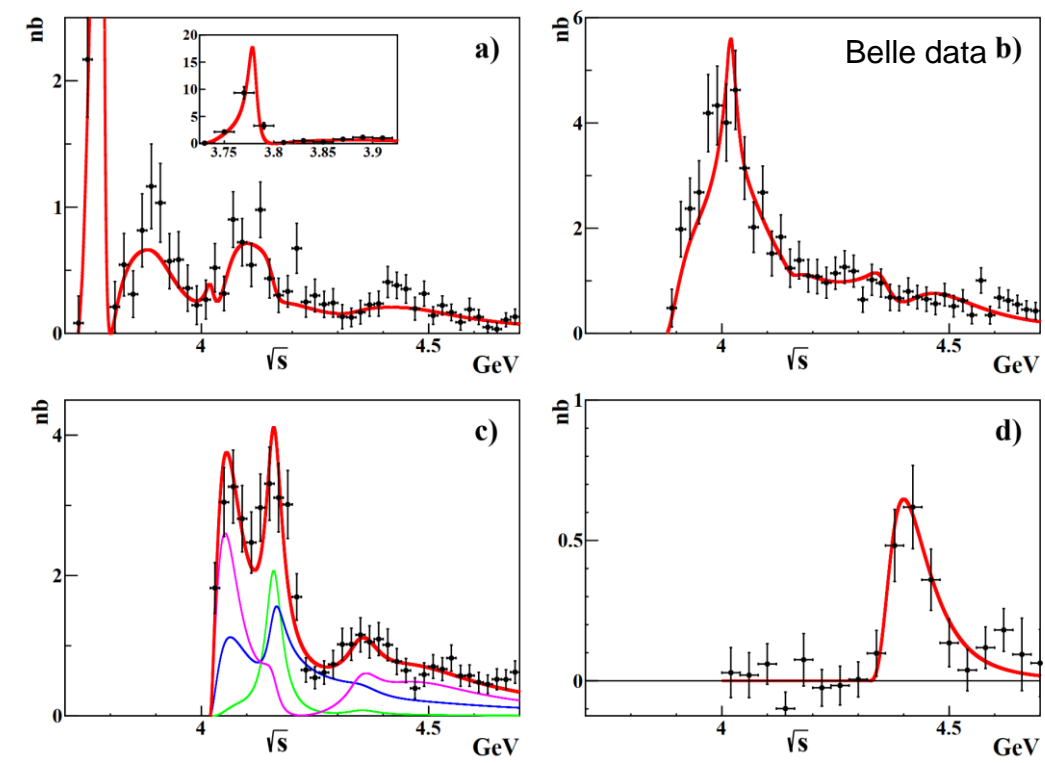


Figure 1. Exclusive cross sections for the $e^+e^- \rightarrow D\bar{D}$ ($[e^+e^- \rightarrow D^+D^-] + [e^+e^- \rightarrow D^0\bar{D}^0]$) (plot (a)), $e^+e^- \rightarrow D^*D^{*-}$ (plot (b)), $e^+e^- \rightarrow D^{*+}D^{*-}$ (plot (c)), and $e^+e^- \rightarrow D\bar{D}\pi$ ($[e^+e^- \rightarrow D^0D^-\pi^+] + [e^+e^- \rightarrow \bar{D}^0D^+\pi^-]$) (plot (d)). In all plots, the points with the error bars represent the Belle data [41] and the red curves show the fit results. In plot (c), the blue, magenta and green thin curves represent the P -wave with $S = 0$, the P -wave with $S = 2$, and the F -wave with $S = 2$ contributions in $D^{*+}D^{*-}$ final state, respectively.



Background

Gamow态的数学基础

Energy eigenfunction with a complex eigenvalue, proposed by G.Gamow to understand alpha decay.

G.Gamow , Z.Phys. 51 (1928) 204-212

However, in Hilbert space, a self-adjoint operator can only admit real eigenvalues. A rigorous treatment to Gamow state require an extension of Hilbert space to Rigged Hilbert space(RHS).

Friedrichs-Lee 模型 A.Bohm, M.Gadella, Dirac kets, Gamow vectors, and Gelfund Triplets, Springer Lectures Notes in Physics Vol.348, Springer, Berlin

A solvable model to demonstrate the properties of Gamow state.

Several variants: K. O. Friedrichs, Communications on Pure and Applied Mathematics 1, 361 (1948).

Lee model T. D. Lee, Phys. Rev. 95, 1329 (1954),

Fano model U. Fano, Phys. Rev. 124, 1866 (1961).

Anderson model P. W. Anderson, Phys. Rev. 124, 41 (1961).



Background

Free Hamiltonian H_0 with a simple continuous spectrum $R^+ \equiv [0, \infty)$, and a discrete eigenstate $|1\rangle$ with the eigenvalue $\omega_0 > 0$.

$$H_0 |1\rangle = \omega_0 |1\rangle, H_0 |\omega\rangle = \omega |\omega\rangle$$

Then the free Hamiltonian is

$$H_0 = \omega_0 |1\rangle\langle 1| + \int_0^\infty d\omega \omega |\omega\rangle\langle\omega|$$

Normalization :

$$\langle 1 | 1 \rangle = 1, \langle 1 | \omega \rangle = \langle \omega | 1 \rangle = 0, \langle \omega' | \omega \rangle = \delta(\omega' - \omega)$$

Suppose there is an interaction between the continuous and discrete parts

$$V = \lambda \int_0^\infty d\omega [f(\omega) |\omega\rangle\langle 1| + f^*(\omega) |1\rangle\langle\omega|]$$



Background

We can solve the eigenstate $|\Psi(x)\rangle$ of the full Hamiltonian $H = H_0 + V$, with eigenvalue x .

$$H |\Psi(x)\rangle = x |\Psi(x)\rangle$$

Since the $|1\rangle$ and $|\omega\rangle$ form a complete set, $|\Psi(x)\rangle$ could be expressed as

$$|\Psi(x)\rangle = \alpha(x) |1\rangle + \int_0^\infty d\omega \varphi(x, \omega) |\omega\rangle$$

Using

$$V|1\rangle = \lambda f(\omega) |\omega\rangle, V|\omega\rangle = \lambda f^*(\omega) |1\rangle$$

We have

$$(\omega_0 - x)\alpha(x) + \lambda \int_0^\infty f^*(\omega) \psi(x, \omega) d\omega = 0,$$

$$(\omega - x)\psi(x, \omega) + \lambda f(\omega)\alpha(x) = 0.$$



Background

For Eigenvalue

$$x > 0$$

$$\psi_{\pm}(x, \omega) = -\frac{\lambda \alpha(x) f(\omega)}{\omega - x \pm i\varepsilon} + \gamma_{\pm}(\omega) \delta(\omega - x),$$

$$(\omega_0 - x) \alpha_{\pm}(x) + \lambda f^*(x) \gamma_{\pm}(x) - \alpha_{\pm}(x) \lambda^2 \int_0^{\infty} \frac{f(\omega) f^*(\omega)}{\omega - x \pm i\varepsilon} d\omega = 0.$$

Define resolvent function

$$\eta^{\pm}(x) = x - \omega_0 - \lambda^2 \int_0^{\infty} \frac{|f(\omega)|^2}{x - \omega \pm i\varepsilon} d\omega$$

Solution:

$$|\Psi(x)\rangle = |x\rangle + \lambda \frac{f^*(x)}{\eta^{\pm}(x)} [|1\rangle + \lambda \int_0^{\infty} \frac{f(\omega)}{x - \omega \pm i\varepsilon} |\omega\rangle d\omega]$$



Two-pole structure(双极点结构) resolvent function

$$\eta(s) = s - \omega_0^2 - \int_{sth} ds' \frac{\rho(s')}{s - s' + i\epsilon}$$

$$\rho(s) \equiv 2\omega_0 \frac{kE_1 E_2}{\sqrt{s}} \alpha(k)^2$$

双极点结构：一个裸态产生两个共振极点。

Phys.Rev.D 83 (2011) 014010

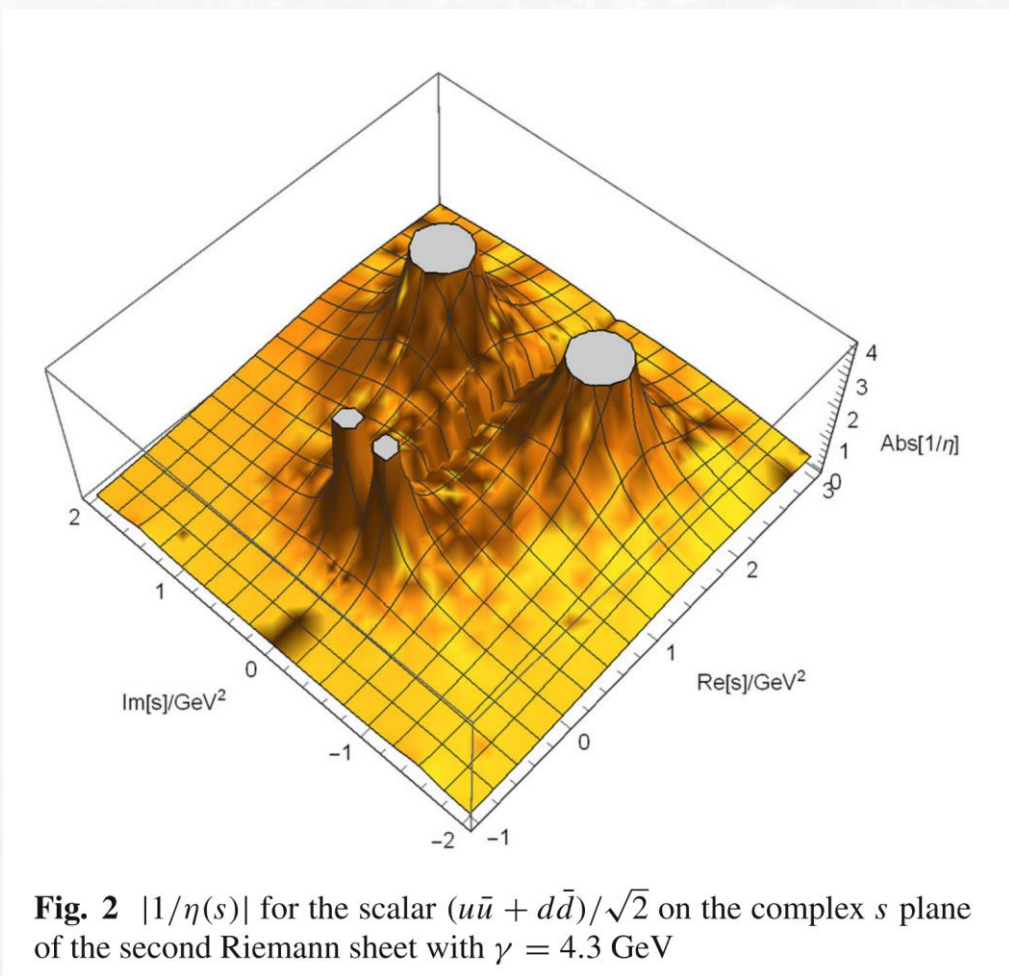
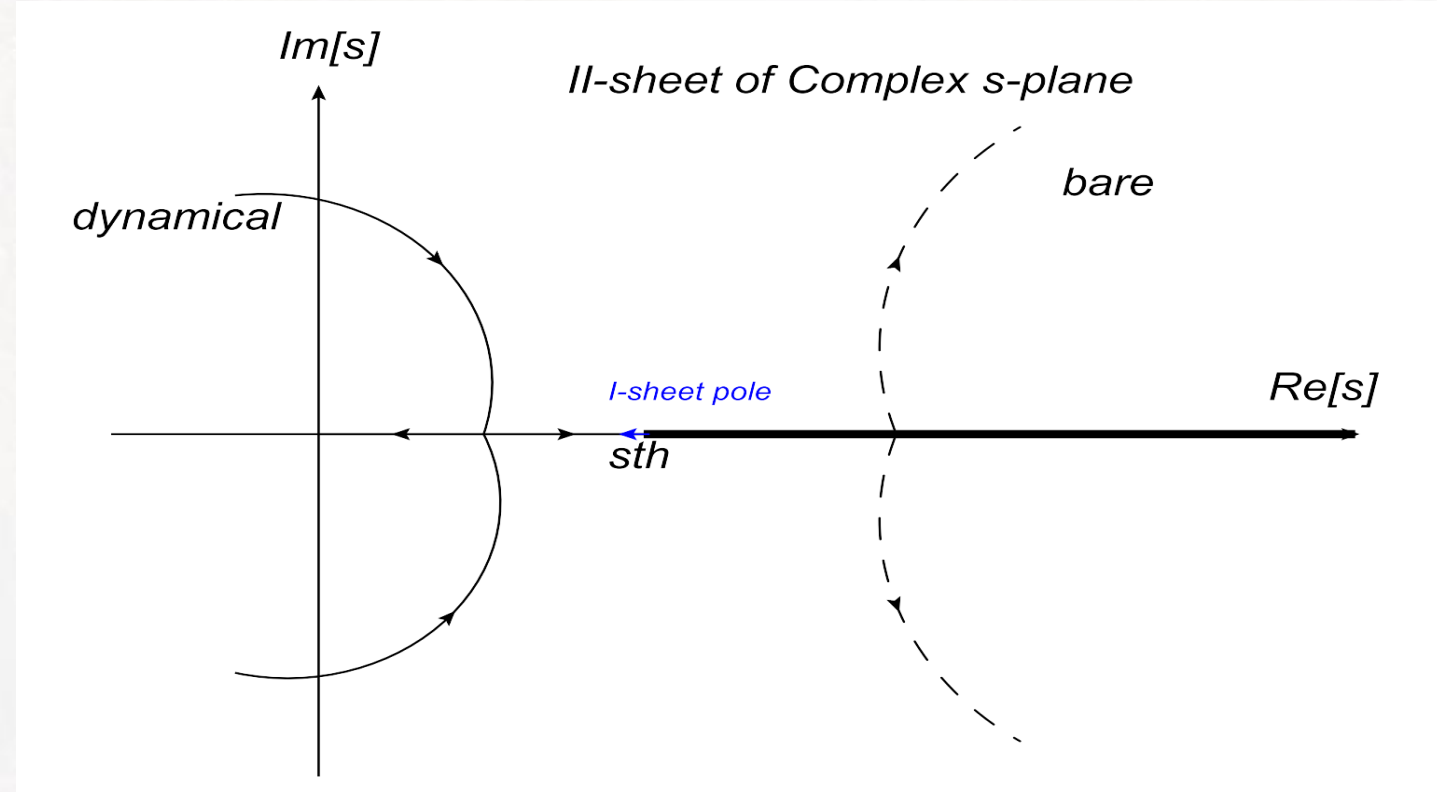


Fig. 2 $|1/\eta(s)|$ for the scalar $(u\bar{u} + d\bar{d})/\sqrt{2}$ on the complex s plane of the second Riemann sheet with $\gamma = 4.3$ GeV

Eur.Phys.J.C 80 (2020) 12, 1191
Eur.Phys.J.C 81 (2021) 6, 551



Two-pole structure(双极点结构)



The general trajectories of two pairs of poles for the two-pole structures on the second Riemann sheet of the s -plane as γ increases.

Eur.Phys.J.C 80 (2020) 12, 1191
Eur.Phys.J.C 81 (2021) 6, 551



Sum rule:

This kind of two-pole structure contribute a total phase shift of 180° in the single channel approximation

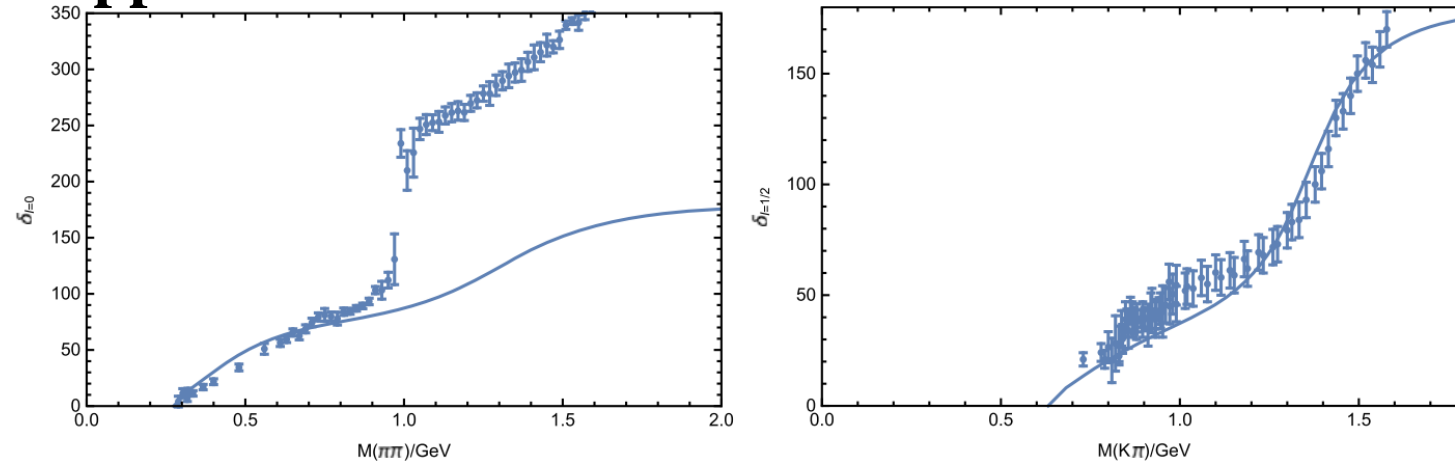


Fig. 3 Comparisons of experimental phase shifts and the theoretical calculations when $\gamma = 4.3 \text{ GeV}$. The left one is that of $IJ = 00 \pi\pi$ scattering and the right one is that of $IJ = \frac{1}{2}0 \pi K$ scattering. The solid line is the contribution of two-pole structure



猜测：双极点结构的普遍性

An ambitious prediction with only a few parameters in this scheme

(1) Some Bare Masses (2) a global coupling γ

Table 1 Correspondence of the discrete states and the continuum states as the parameter $\gamma = 4.3 \text{ GeV}$. The values in the fourth column are the input mass of bare states. Unit is GeV

“Discrete”	“Continuum”	GI mass	Input	Poles	Experiment states	PDG values [19]
$\frac{u\bar{u}+d\bar{d}}{\sqrt{2}}(1^3P_0)$	$(\pi\pi)_{I=0}$	1.09	1.3	$\sqrt{s_{r1}} = 1.34 - 0.29i$	$f_0(1370)$	$1.35^{+0.15} - 0.2^{+0.05}i$
				$\sqrt{s_{r2}} = 0.39 - 0.26i$	$f_0(500)$	$0.475^{+0.075} - 0.275^{+0.075}i$
$u\bar{s}(1^3P_0)$	$(\pi K)_{I=\frac{1}{2}}$	1.23	1.42	$\sqrt{s_{r1}} = 1.41 - 0.17i$	$K_0^*(1430)$	$1.425^{+0.05} - 0.135^{+0.04}i$
				$\sqrt{s_{r2}} = 0.66 - 0.34i$	$K_0^*(700)$	$0.68^{+0.05} - 0.30^{+0.04}i$
$s\bar{s}(1^3P_0)$	$K\bar{K}$	1.35	1.68	$\sqrt{s_{r1}} = 1.71 - 0.16i$	$f_0(1710)$	$1.704^{+0.012} - 0.062^{+0.009}i$
				$\sqrt{s_b} = 0.98, \sqrt{s_v} = 0.19$	$f_0(980)$	$0.99^{+0.02} - 0.028^{+0.023}i$
$\frac{u\bar{u}-d\bar{d}}{\sqrt{2}}(1^3P_0)$	$\pi\eta$	1.09	1.3	$\sqrt{s_{r1}} = 1.26 - 0.14i$	$a_0(1450)$	$1.474^{+0.019} - 0.133^{+0.007}i$
				$\sqrt{s_{r2}} = 0.70 - 0.42i$	$a_0(980)$	$0.98^{+0.02} - 0.038^{+0.012}i$
$c\bar{u}(1^3P_0)$	$D\pi$	2.4	2.4	$\sqrt{s_{r1}} = 2.58 - 0.24i$	$D_0^*(2300)$	$2.30^{+0.019} - 0.137^{+0.02}i$
				$\sqrt{s_{r2}} = 2.08 - 0.10i$		
$c\bar{s}(1^3P_0)$	DK	2.48	2.48	$\sqrt{s_{r1}} = 2.80 - 0.23i$		
				$\sqrt{s_b} = 2.24, \sqrt{s_v} = 1.8$	$D_{s0}^*(2317)$	$2.317^{+0.0005} - 0.0038^{+0.0038}i$
$b\bar{u}(1^3P_0)$	$\bar{B}\pi$	5.76	5.76	$\sqrt{s_{r1}} = 6.01 - 0.21i$		
				$\sqrt{s_{r2}} = 5.56 - 0.07i$		
$b\bar{s}(1^3P_0)$	$\bar{B}K$	5.83	5.83	$\sqrt{s_{r1}} = 6.23 - 0.17i$		
				$\sqrt{s_b} = 5.66, \sqrt{s_v} = 5.3$		
$c\bar{c}(2^3P_1)$	$D\bar{D}^*$	3.95	3.95	$\sqrt{s_{r1}} = 4.01 - 0.049i$	$X(3940)$	
				$\sqrt{s_b} = 3.785$	$X(3872)$	$3.871^{+0.0017}_{-0.0017}$

Eur.Phys.J.C 80 (2020) 12, 1191
 Eur.Phys.J.C 81 (2021) 6, 551



猜测：双极点结构的普遍性

An ambitious prediction with only a few parameters in this scheme

(1) Some Bare Masses (2) a global coupling γ

results of $\gamma = 3.0 \text{GeV}$

$c\bar{u}(1^3P_0)$	$\sqrt{s_{r1}} = 2.39 - 0.18i$	$\sqrt{s_{r2}} = 2.21 - 0.28i$	$D_0^*(2300)$
$c\bar{s}(1^3P_0)$	$\sqrt{s_{r1}} = 2.68 - 0.26i$	$\sqrt{s_b} = 2.32, \sqrt{s_v} = 1.9$	$D_{s0}^*(2317)$
$b\bar{u}(1^3P_0)$	$\sqrt{s_{r1}} = 5.85 - 0.26i$	$\sqrt{s_{r2}} = 5.62 - 0.13i$	
$b\bar{s}(1^3P_0)$	$\sqrt{s_{r1}} = 6.11 - 0.22i$	$\sqrt{s_b} = 5.72, \sqrt{s_v} = 5.4$	
$c\bar{c}(2^3P_1)$	$\sqrt{s_r} = 3.99 - 0.05i$	$\sqrt{s_b} = 3.84$	$X(3872)$

Notice that it is a prediction with only one parameter γ .



多粒子多道的Friedrichs-Lee-QPC框架

Hamiltonian

$$H_0 = \sum_{\rho=1}^D M_\rho |\rho\rangle\langle\rho| + \sum_{i=1}^C \int_{a_i}^{\infty} d\omega E |E; i\rangle\langle E; i|,$$

$$V = \sum_{\rho=1}^D \sum_{i=1}^C \int_{a_i}^{\infty} dE [f_{\rho i}^*(E) |\rho\rangle\langle E; i| + f_{\rho i}(E) |E; i\rangle\langle \rho|].$$

Scattering matrix

$$S_{i,j} = \delta_{ij} - 2\pi i \sum_{\lambda} f_{\rho j}^*(E) [\eta^{-1}]_{\rho \lambda} f_{\lambda i}(E)$$

$$[\eta]_{\rho \lambda} \equiv (E - M_\rho) \delta_{\rho \lambda} - \sum_{i=1}^C \int_{a_i}^{\infty} dE' \frac{f_{\rho i}^*(E') f_{\lambda i}(E')}{(E - E')}$$

ψ coupling to hadron pairs

QPC model

ψ coupling to $e^+ e^-$

$$\mathcal{M}(\psi_\rho \rightarrow e^+ e^-) = \frac{e g_{e\rho}}{M_\rho^2} (\bar{u} \gamma_\mu v) \epsilon^\mu,$$

Cross section of $e^+ e^- \rightarrow$ hadron pairs

$$\sigma_i(E) = \frac{32\pi^5 \alpha}{E^5} \left| \sum_{\rho \lambda} g_{e\rho} [\eta^{-1}]_{\rho \lambda} f_{\lambda i} \right|^2$$



多粒子多道的Friedrichs-Lee-QPC框架拟合

4 channels

$$e^+e^- \rightarrow D\bar{D}, D\bar{D}^*, D^*\bar{D}^*, D\bar{D}\pi$$

4 bare discrete states are supposed

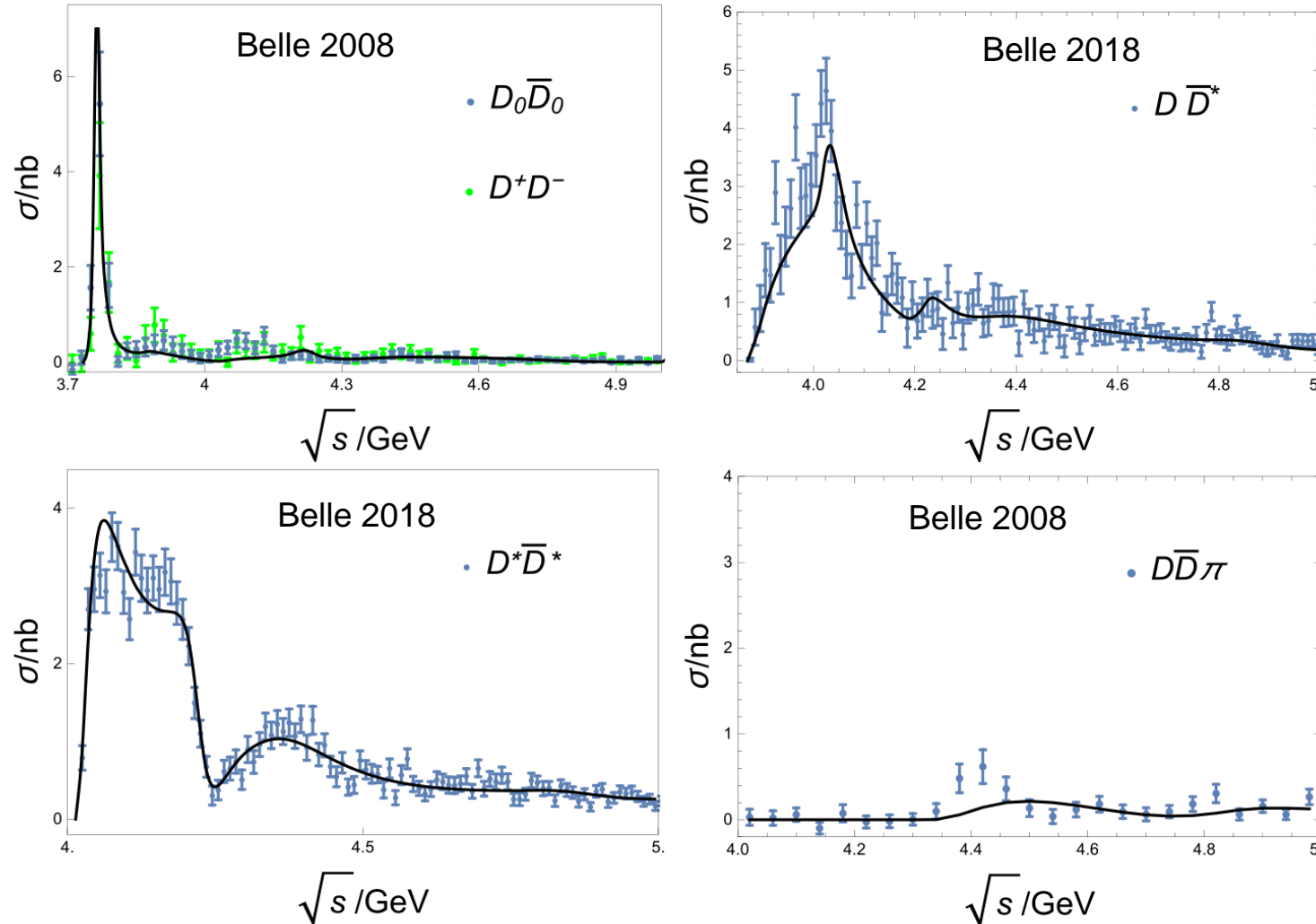
$$\psi(1D), \psi(3S), \psi(2D), \psi(4S)$$

15 parameters

	Background	$\psi(1D)$	$\psi(3S)$	$\psi(2D)$	$\psi(4S)$
Bare mass	1.83	4.09	4.36	4.62	5.35
$g_{e\rho}$	26.4	1.82	5.32	-3.68	-6.12
$\phi_{e\rho}/^\circ$	0(fixed)	35.2	-31.6	64.6	129.3
γ		4.48			



Combined fit of $e^+e^- \rightarrow D\bar{D}, D\bar{D}^*, D^*\bar{D}^*, D\bar{D}\pi$



$$\frac{\chi^2}{d.o.f} = \frac{379}{293-15} \sim 1.36$$

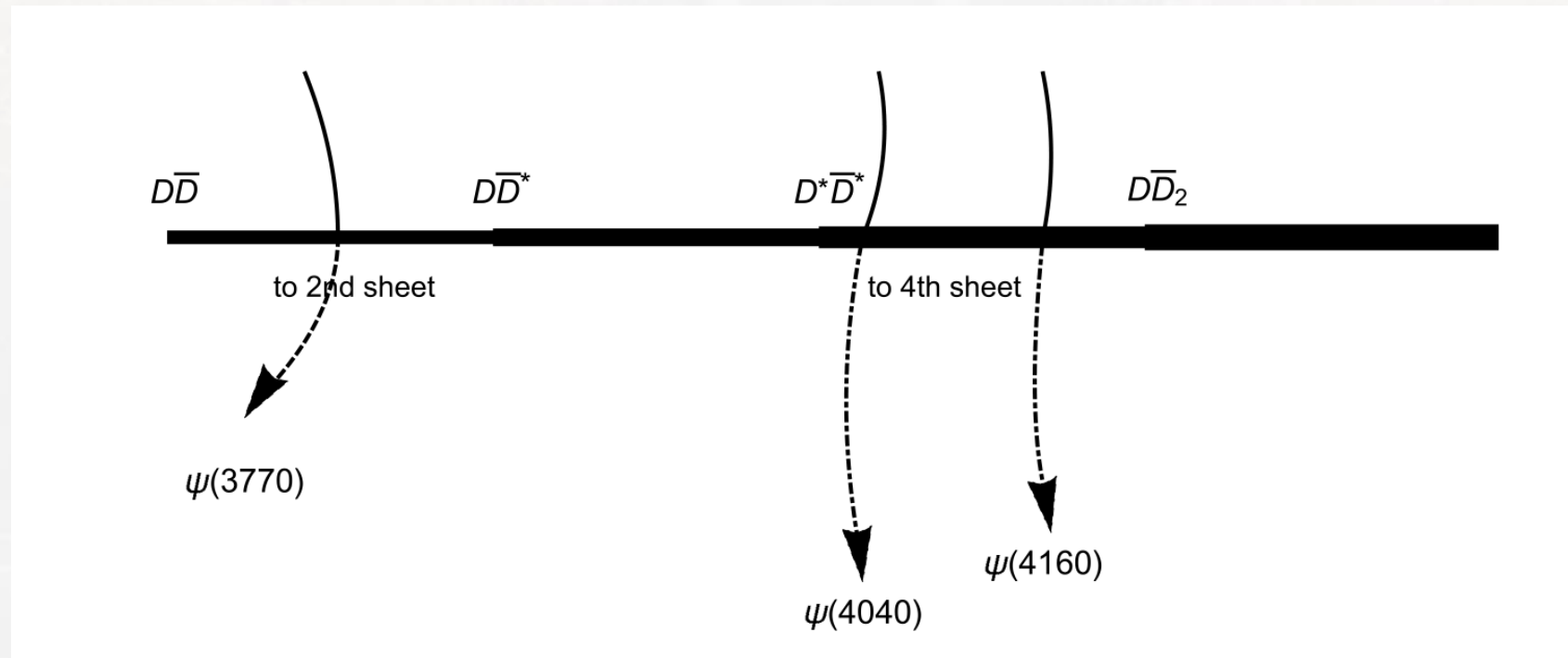


Extract the nearby poles

4 channels

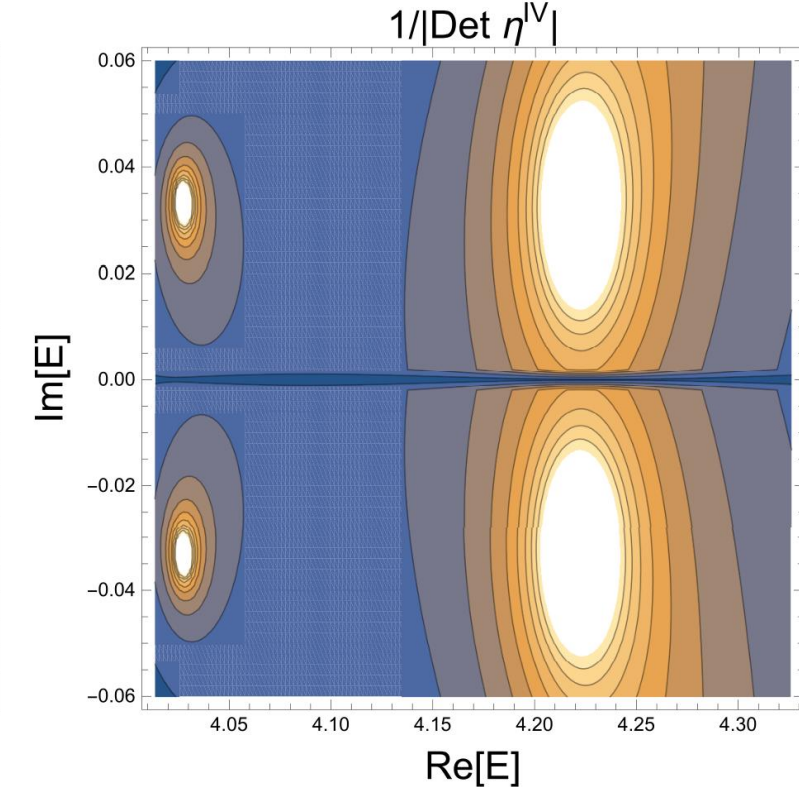
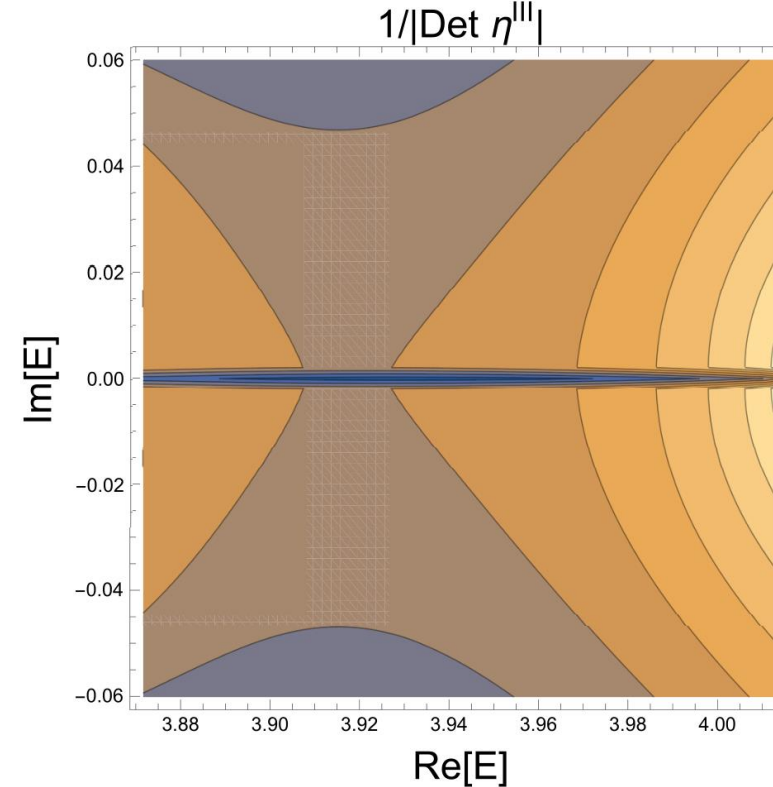
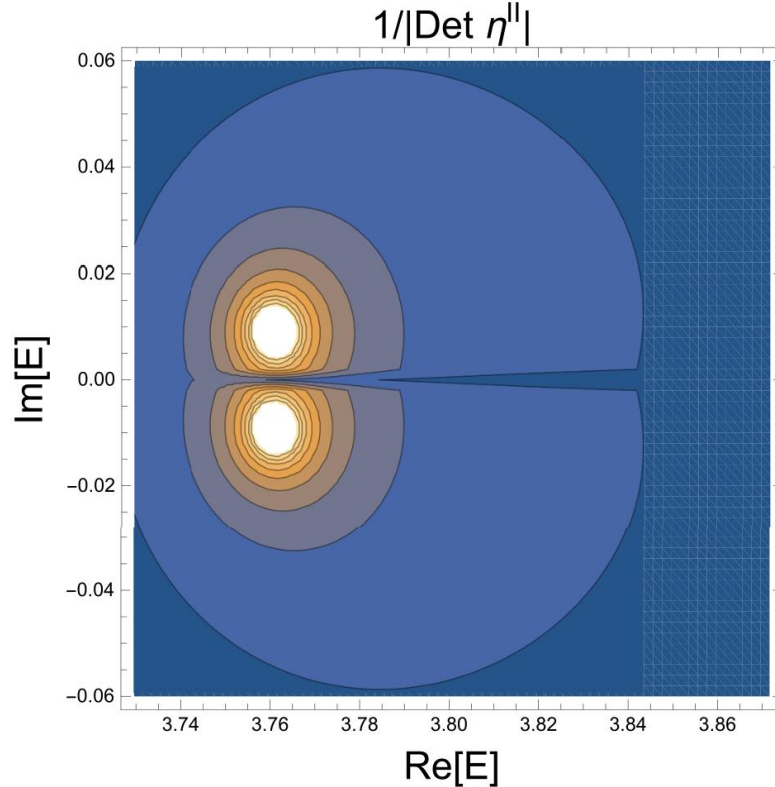
16 Riemann sheets

Extract the nearby poles by find the solution of $\det[\eta^{(N\text{-sheet})}] = 0$





Contour plots of $1/\det[\eta]$ on unphysical Riemann sheets



$$z_0^{II} = 3.762 - \frac{0.020}{2} i \text{ GeV}$$

$\psi(3770)$

A shadow pole above $D^*\bar{D}^*$,
 $\psi(4008)???$

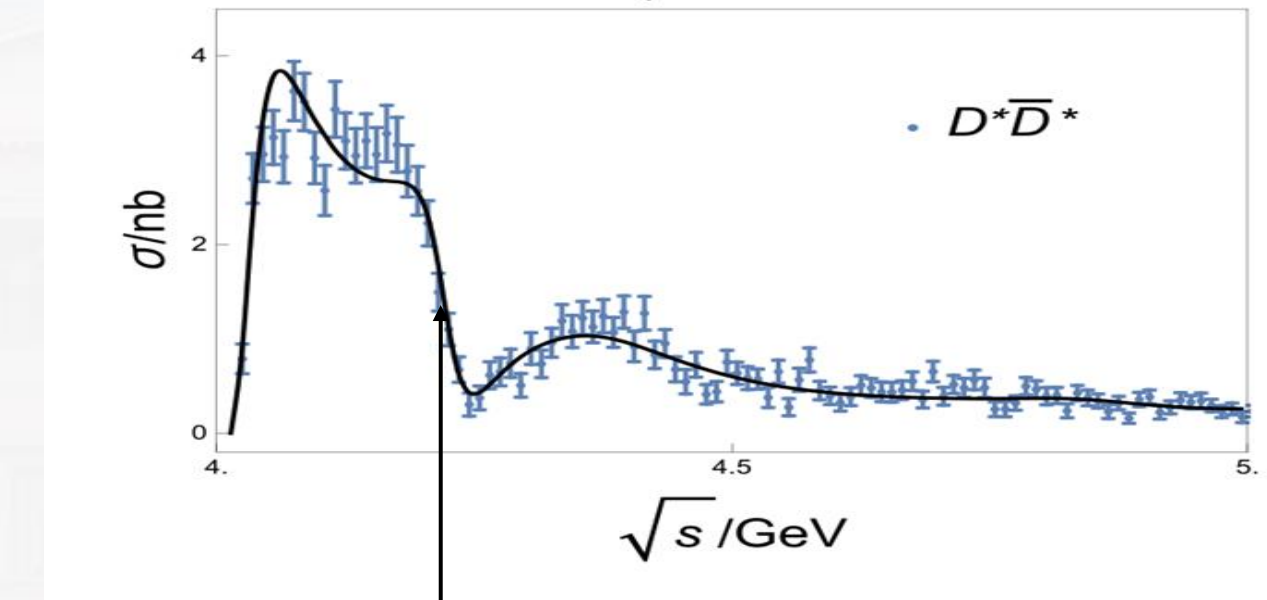
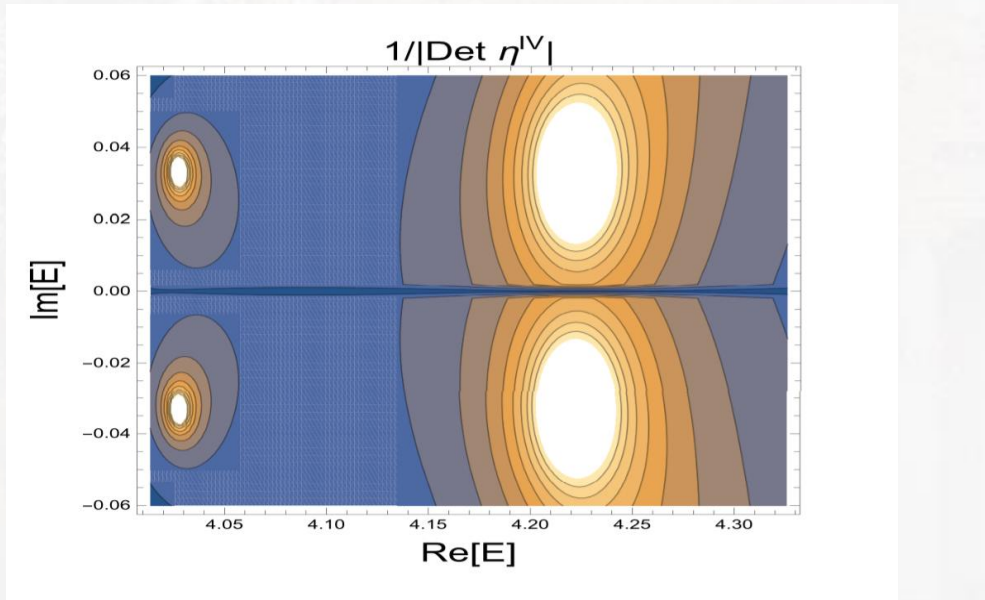
$$z_{0,1}^{IV} = 4.028 - \frac{0.068}{2} i \text{ GeV} \quad \psi(4040)$$

$$z_{0,2}^{IV} = 4.222 - \frac{0.064}{2} i \text{ GeV}$$

$$\psi(4160)/\psi(4230)$$



Contour plots of $1/\det[\eta]$ on 4-th sheet



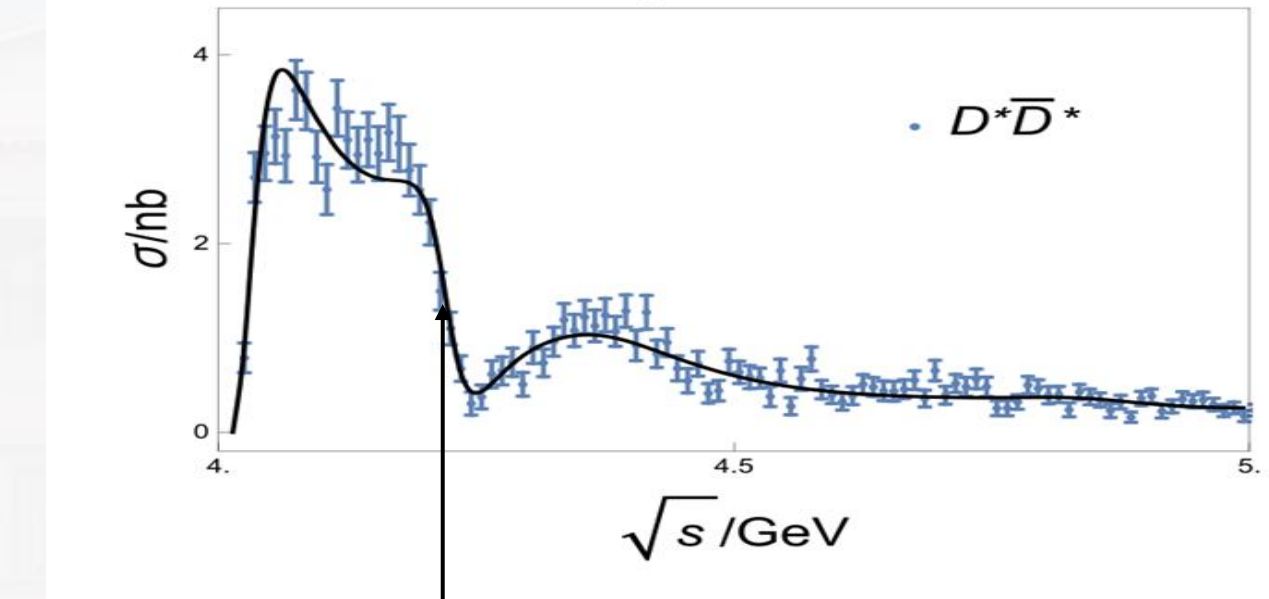
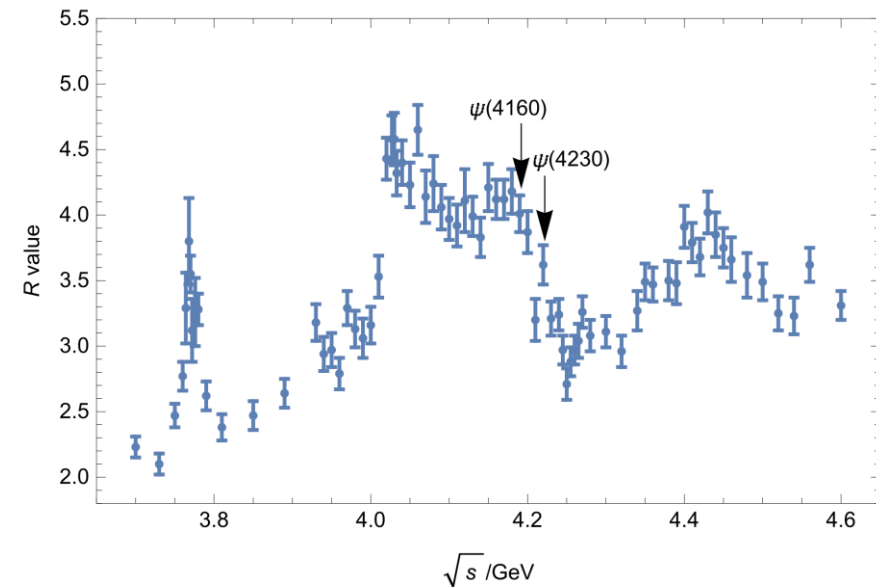
$$z_{0,2}^{IV} = 4.222 - \frac{0.064}{2} i \text{ GeV}$$

$$\psi(4160)/\psi(4230)$$

at the half hillside of sharp declined cross section, neither at the shoulder nor at the dip



Contour plots of $1/\det[\eta]$ on 4-th sheet



$$z_{0,2}^{IV} = 4.222 - \frac{0.064}{2} i \text{ GeV}$$

$\psi(4160)/\psi(4230)$

at the half hillside of sharp declined cross section, neither at the shoulder nor at the dip



If $\psi(4160)$ and $\psi(4230)$ are the same $\psi(2^3D_1)$ state
benefits

- Quark model expectation
- Explanation of the mutually exclusive decay modes of $\psi(4160)$ and $\psi(4230)$
- Reliability of coupled channel method analysis

Challenges faced in verifying this conjecture

- A fit with more bare discrete states and more decay model
 $D\bar{D}, D\bar{D}^*, D^*\bar{D}^*, D\bar{D}_1, D\bar{D}_2^*, D_s^+D_s^-, D_s^+D_s^{*-}, D_s^{*+}D_s^{*-}, \dots \dots$
- More accurate experiment data



Expected experiment explorations

More precise $J/\psi\eta$ data

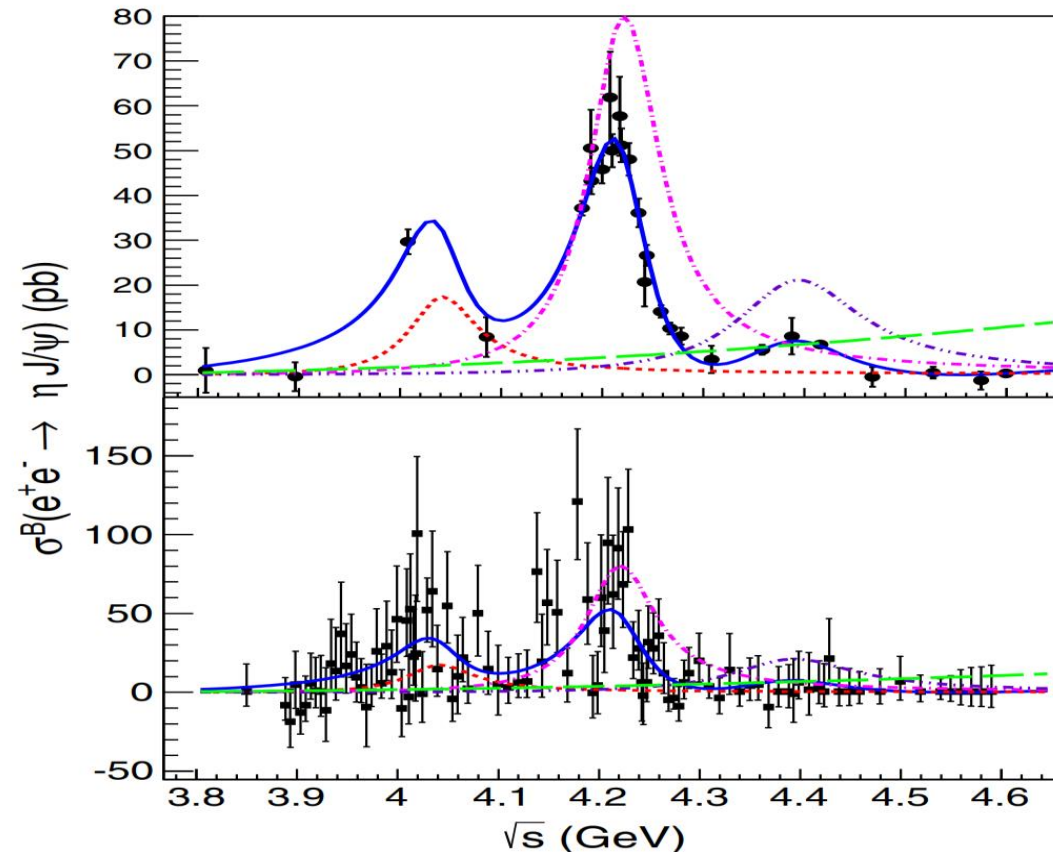


FIG. 2. Top: Cross section and fits of $e^+e^- \rightarrow \eta J/\psi$ for XYZ data. Bottom: Same for the scan data. Dots with error bars are data. The solid (blue) curves represent the fit results of the

BES,
PRD 102, 031101



Expected experiment explorations

More precise $D_s^{(*)+} D_s^{*-}$ data

Belle, PRD 83, 011101(R) (2011)

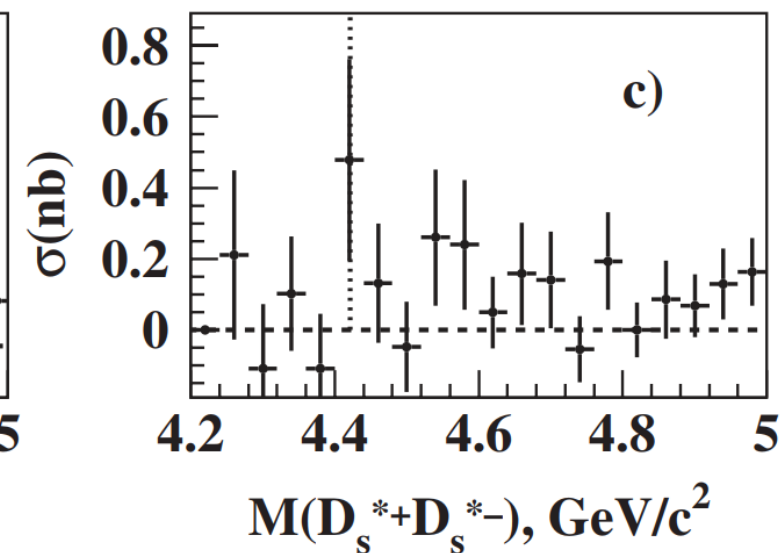
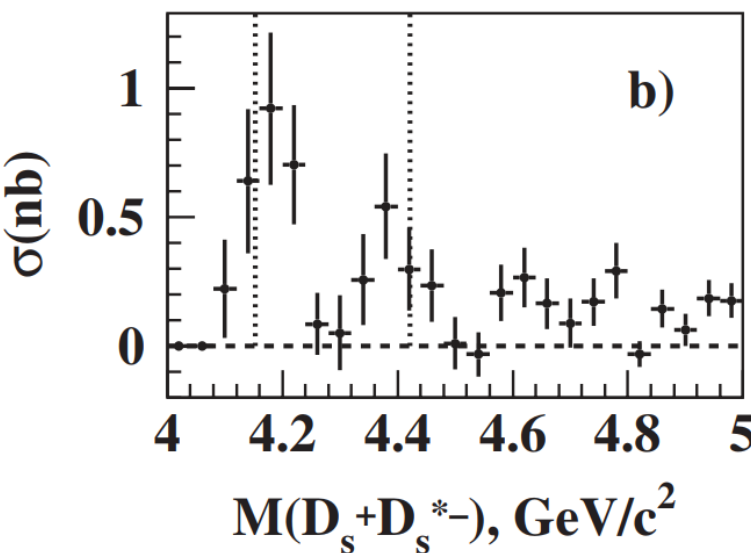
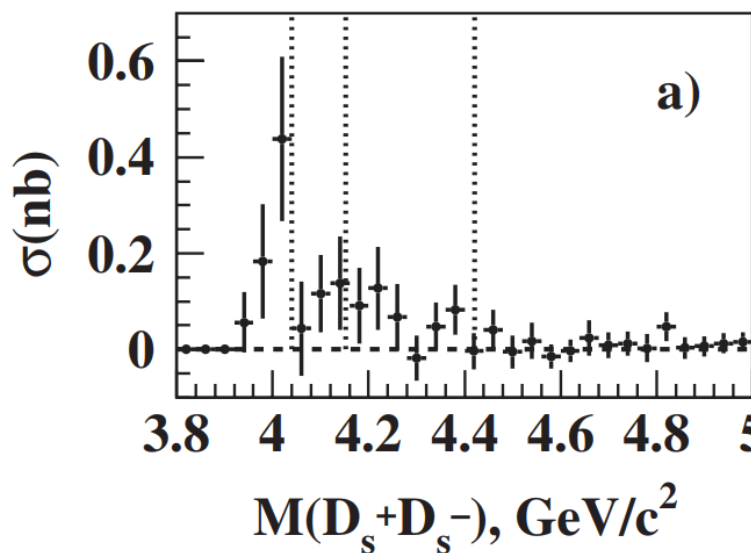
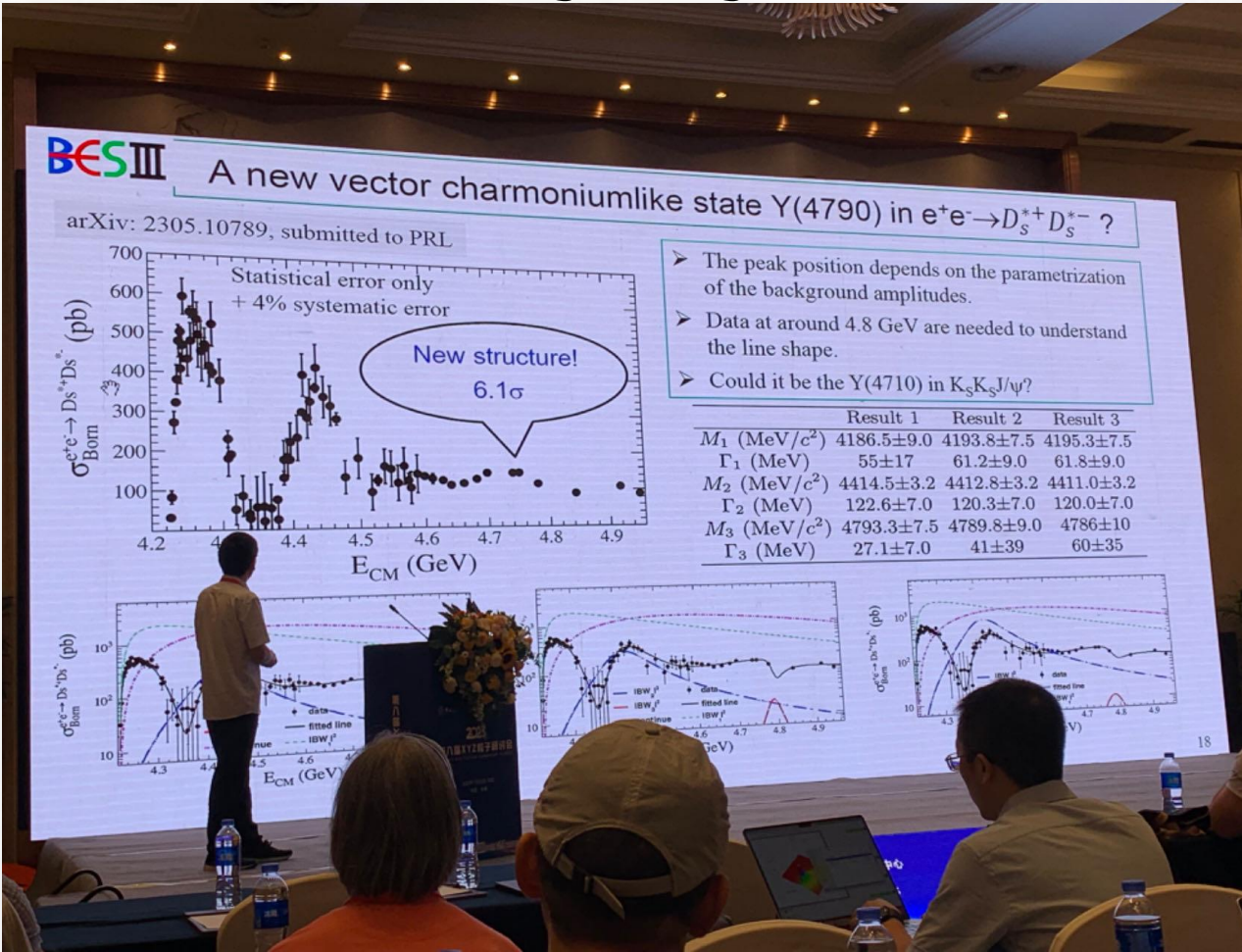


FIG. 4. The cross section averaged over the bin width for (a) the $e^+e^- \rightarrow D_s^+ D_s^-$ process, (b) the $e^+e^- \rightarrow D_s^+ D_s^{*-} + \text{c.c.}$ process, and (c) the $e^+e^- \rightarrow D_s^{*+} D_s^{*-}$ process. Error bars show statistical uncertainties only. There is a common systematic uncertainty for all measurements, 11% for $D_s^+ D_s^-$, 17% for $D_s^+ D_s^{*-}$, and 31% for $D_s^{*+} D_s^{*-}$. This uncertainty is described in the text. The dotted lines show masses of the $\psi(4040)$, $\psi(4160)$, and $\psi(4415)$ states [18].



Expected experiment explorations

More precise $D_s^{(*)+} D_s^{*-}$ data



Prof. Yuan's talk
2023.7.26

BES, arxiv: 2305.10789



- $\psi(4160)$ and $\psi(4230)$ might be the same $\psi(c\bar{c} \, 2^3D_1)$ state.
- More experiments such as $J/\psi\eta$ and $D_s^{(*)}\bar{D}_s^{(*)}$ are required to verify or falsify the conjecture.
- We present a coupled-channel scheme with unitarity and analyticity, which could be used to study several resonances and several decay modes simultaneously.
- This scheme could be rewritten into the form used in the experimental analysis.



Thanks for your
patience!

